Quantum Electronics **50** (6) 566–570 (2020)

https://doi.org/10.1070/QEL17352

Detection of the clock transition in thulium atoms by using repump laser radiation

D.O. Tregubov, A.A. Golovizin, E.S. Fedorova, D.A. Mishin, D.I. Provorchenko, K.Yu. Khabarova, V.N. Sorokin, N.N. Kolachevsky

Abstract. **A population transfer from the upper level of the clock transition in thulium atoms to the ground level is demonstrated by using radiation with a wavelength of 402 nm. The method for detecting the clock transition excitation that is not affected by technical fluctuations of the number of atoms in an optical lattice is investigated. The hyperfine splitting of the $|4f^{12}(^3F_2)5d_{5/2}6s^2; J = 7/2\rangle$ level in the thulium atom is measured to be 1480(9) MHz. The suggested method for population transfer can be applied to both the hyperfine components of the clock transition intended for compensating Zeeman effect in a thulium optical clock.**

Keywords: *spectroscopy, hyperfine splitting, optical clock, clock transition, ultracold atoms, thulium.*

1. Introduction

Presently, modern optical clocks provide the most accurate relative frequency measurements. They are used for testing fundamental theories [1–3] and in applied fields [4]. Optical clocks based on single ions reach a relative error of 9.4×10^{-19} and a relative frequency instability of $1.2 \times 10^{-15}/\sqrt{\tau}$ at an averaging time τ (s) [5]. Optical clocks on neutral atoms have a higher stability and similar relative error as compared to clocks on single ions [6, 7]. This is especially important for transportable clocks outside laboratories when the time needed for performing measurements and achieving the required accuracy should be minimal.

The employment of transportable optical clocks opens a possibility of charting maps of the Earth gravitational field [8] and using these devices in satellite positioning [9]. Optical clocks based on neutral thulium atoms form an attractive basis for transportable clocks because the clock transition exhibits a low sensitivity to thermal emission and static electric fields unlike neutral atoms [10–12]. This eases temperature control requirements for the environment and simplifies the construction of a system.

The relative instability of a clock frequency ν determined by the standard quantum noise limit depends on the signal averaging time τ according to the formula [13]

$$\sigma(\tau) = \frac{\delta\nu}{\nu}\frac{\xi}{(\mathrm{S/N})\sqrt{\tau}}, \qquad (1)$$

where ξ is the dimensionless parameter close to unity related to the method of atomic transition interrogation; $\delta\nu$ is the detected spectral width for the transition at frequency ν; and S/N is the signal-to-noise ratio, that is, the ratio of the probability for resonant excitation of the clock transition to the inaccuracy of determining this probability.

In previous papers [10, 14–16] devoted to thulium optical lattice clock, the probabilty of the clock transition excitation was calculated from the number of atoms at the ground state under the assumption that the total number of atoms remains constant throughout the experiment. However, there are fluctuations of the number of particles, which may both deteriorate the signal-to-noise ratio and shift the line centre due to an incorrectly determined error signal used for stabilising the clock laser frequency.

The transition excitation probability can be determined more accurately by using two numbers obtained from a single measurement cycle (the number of atoms at the ground state and at upper level of the clock transition), similarly to optical clocks based on strontium and ytterbium atoms [17, 18] and on atomic fountains [19]. Therefore, a controlled mechanism of atom return from the upper clock level to the ground state is needed without employing the clock laser radiation. Such a mechanism may be atom excitation from the upper level of the clock transition to the level from which atoms mainly decay to the ground state in a short time as compared to the clock level lifetime. For this purpose, the transition with a wavelength of 402 nm to the level $|\mathrm{r}\rangle = |4f^{12}(^3F_2)5d_{5/2}6s^2; J = 7/2\rangle$ [20] was chosen. The probability of the dipole transition from this level to the ground state is $A_{\mathrm{gr}} = 2.17 \times 10^7\ \mathrm{s}^{-1}$ and to the clock level is $A_{\mathrm{cr}} = 4.5 \times 10^5\ \mathrm{s}^{-1}$.

2. Spectroscopy of the transition for population transfer

Optical repumping of thulium atoms was studied by using a diode laser. According to information from the manufacturer (VitaWave), the radiation spectral width of about 1 MHz is determined by an external laser cavity. The laser frequency

D.O. Tregubov, A.A. Golovizin, E.S. Fedorova, D.A. Mishin, D.I. Provorchenko, V.N. Sorokin Lebedev Physical Institute, Russian Academy of Sciences, Leninsky prosp. 53, 119991 Moscow, Russia; e-mail: treg.dim@gmail.com;
K.Yu. Khabarova, N.N. Kolachevsky Lebedev Physical Institute, Russian Academy of Sciences, Leninsky prosp. 53, 119991 Moscow, Russia; Russian Quantum Centre, Bol'shoi bul., 30, stroenie 1, Skolkovo, 121205 Moscow, Russia;
e-mail: kseniakhabarova@gmail.com

Received 11 March 2020; revision received 1 April 2020
Kvantovaya Elektronika **50** (6) 566–570 (2020)
Translated by N.A. Raspopov

was stabilised by a WSU-30 wavelength meter (Angstrom). The feedback was realised by applying the corresponding error signal to a piezoelectric actuator of the laser diffraction grating. The system of frequency stabilisation with the wavelength meter made it possible to scan the laser frequency in a range of several gigahertz and study excitation spectra of thulium atoms in a wide spectral band. According to the database [20], the resonance frequency of the repump transition is 745060.3(9) GHz disregarding the hyperfine splitting. The nuclear spin of the only stable thulium isotope is $I = 1/2$, which leads to a dublet hyperfine structure. In an optical clock on thulium atoms, it is assumed to employ two hyperfine components of the clock transition $|g, 4\rangle \rightarrow |c, 3\rangle$ and $|g, 3\rangle \rightarrow |c, 2\rangle$ for cancelling the quadratic Zeeman effect for the mean frequency of two transitions (here, $|c, N\rangle = |4f^{13}(^2F^o)6s^2; J = 5/2, F = N\rangle$ and $|g, N\rangle = |4f^{13}(^2F^o)6s^2; J = 7/2, F = N\rangle$). Therefore, both hyperfine components $|r, 4\rangle$ and $|r, 3\rangle$ of the $|r\rangle$ level should be excited. All the levels of the thulium atom involved in the present work are shown in Fig. 1a.

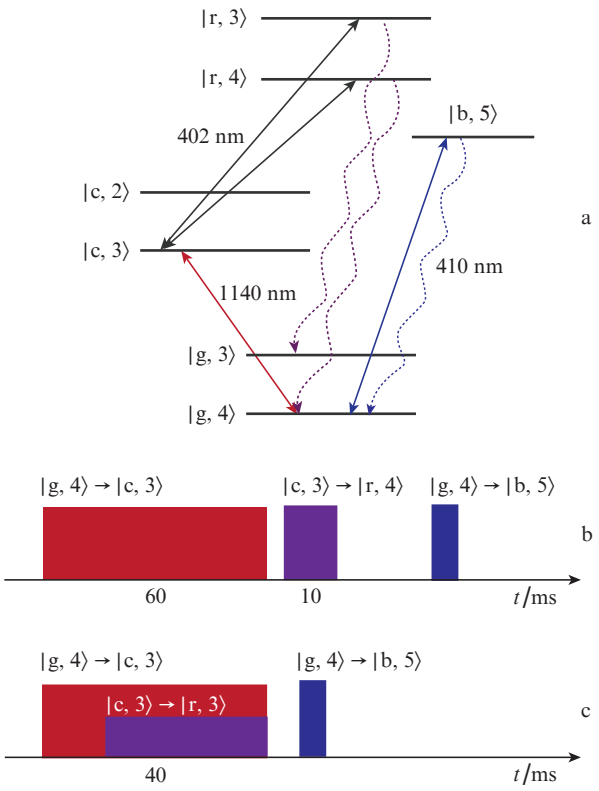

Figure 1. (a) Energy level diagram of thulium atoms and (b, c) pulse sequences with indicated durations for determining the energy level (b) $|r, 4\rangle$ and (c) $|r, 3\rangle$. Level notations: $|g, 4\rangle$ is the ground level for thulium; $|c, 3\rangle$ and $|c, 2\rangle$ are the upper levels of the clock transition; $|r, 4\rangle$ and $|r, 3\rangle$ are the auxiliary levels for population transfer, which are studied in the present work; $|b, 5\rangle$ is the level used for the first cooling stage used for measuring the number of atoms. The radiation pulses of duration 0.2 ms with a wavelength of 410 nm, which are resonant to the $|g, 4\rangle \rightarrow |b, 5\rangle$ transition, are used for determining the number of atoms.

In all experiments discussed below, a cloud of thulium atoms was prepared in a magneto-optical trap (MOT) in two stages of laser cooling and was recaptured into an optical lattice (see, for example, [14–16]). In the present work, an optical lattice was operated at a wavelength of 1064 nm which, according to results from [10], is near a magic wavelength resides for the lattice polarisation direction normal to the quantisation axis defined by the magnetic field. The number of atoms in the ground state $|g, 4\rangle$ was found from a luminescence signal from atoms under excitation of the 410 nm transition to the level $|b, 5\rangle = |4f^{12}(^3H_5)5d_{3/2}6s^2; J = 9/2, F = 5\rangle$, measured with a CMOS camera. It is a destructive method because atoms leave the trap as a result of multiple photon scattering while interacting with the resonant radiation at 410 nm.

The frequencies of transitions $|c, 3\rangle \rightarrow |r, 4\rangle$ and $|c, 3\rangle \rightarrow |r, 3\rangle$, and values of hyperfine splitting of the $|r\rangle$ level were found by using two schemes of the experiment presented in Figs 1b and 1c. In the first scheme, a pulse of the clock laser excites approximately 40% of atoms to the $|c, 3\rangle$ level. The subsequent pulse at a wavelength of 402 nm returns part of the excited atoms back to the ground level. Dotted arrows in Fig. 1a denote the most probable channels of spontaneous decay for each of the hyperfine components of the $|r\rangle$ level. Here, decay to another hyperfine component of the ground level and to the $|c\rangle$ level is 35 and 50 times less probable, respectively. In the case where the 10-ms radiation pulse at 402 nm is in resonance with the $|c, 3\rangle \rightarrow |r, 4\rangle$ transition, some atoms return to the ground state. As a result, an increased number of atoms is observed when luminescence is detected (Fig. 2).

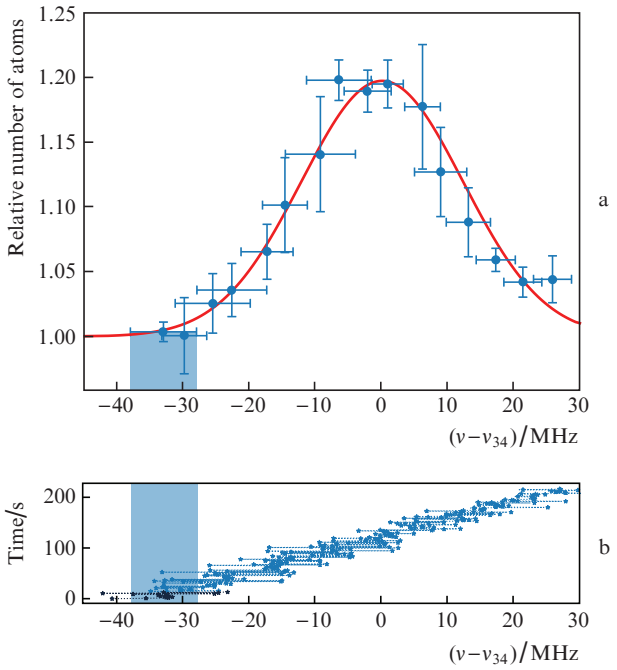

Figure 2. (a) Detection of the $|c, 3\rangle \rightarrow |r, 4\rangle$ transition at a wavelength of 402 nm (near the resonance $\nu \approx \nu_{34}$ the number of atoms at the ground level increases due to atoms returned from the upper clock level); (b) laser radiation frequency and its statistical error determined from wavelength meter readings vs. time.

For obtaining spectra, the following order of operations was realised. A desired value was set in a program for stabilising the radiation frequency of the 402-nm laser. Then a 15-cycle measurement of the excitation efficiency was taken while recording the measured laser frequency (Fig. 2b); from these data, a statistical error of the laser frequency was found (dark points in the figure mark the error of frequency measurement for the first point in the spectrum shown in Fig. 2a).

A frequency of the hyperfine component |c, 3⟩ → |r, 3⟩ was found by using the second scheme shown in Fig. 1c. Atoms excited to the |c, 3⟩ level are repumped through the intermediate level |r, 3⟩ mainly to the |g, 3⟩ sublevel and no longer interact with the clock laser radiation and 410-nm radiation for detecting the number of atoms. Thus, the radiation at 402 nm, which is resonant to the |c, 3⟩ → |r, 3⟩ transition, reduces the number of detected atoms (Fig. 3).

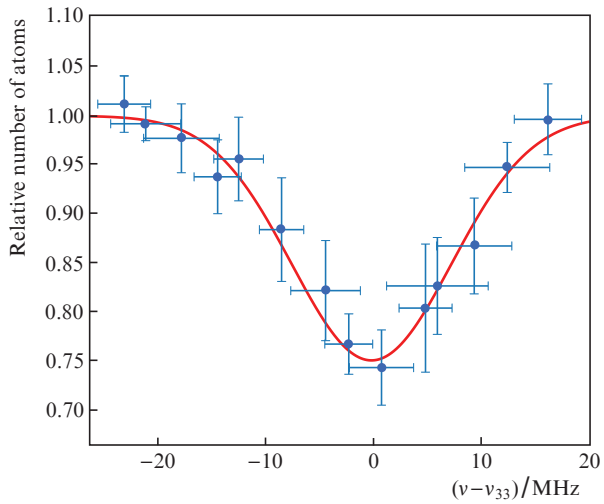

Figure 3. Detection of the |c, 3⟩ → |r, 3⟩ transition at a wavelength of 402 nm (near the resonance frequency ν_{33} the number of atoms at the ground level reduces due to atom transfer to the |g, 3⟩ sublevel). The laser frequency and its statistical error are determined from wavelength meter readings. Approximation by a Gaussian profile (solid curve) yields the value ν_{33} = 745063143.7(5) MHz (the statistical error of approximation is given in parenthesis).

The difference of frequencies in Figs 2 and 3 makes it possible to determine the value of hyperfine splitting which is 1480 MHz.

3. Estimation of measurement error

A statistical error of determining the line centre through approximation of experimental data is 0.7 MHz for the |c, 3⟩ → |r, 4⟩ transition and 0.5 MHz for |c, 3⟩ → |r, 3⟩.

The systematic error is combined from the wavelength measurement error and various shifts of the transition frequency. According to manufacturer, a WSU-30 wavelength metre for 10 hours since the last calibration has an error of 30 MHz for a single-mode fibre and 100 MHz for a multimode fibre. The device resolution is 5 MHz. In the experiment we measured the 410 nm laser radiation frequency using a fibre that is single-mode in the standard transmission window (and multimode for the radiation at 410 nm). It was established that the frequency is reproduced within 5 MHz for a time interval of 1 h. In this case, the laser radiation was stabilised by a high-Q cavity using the Pound–Drever–Hall locking technique [21]. The width of the cavity transmission line is 5 MHz. Analysis of the transmission spectrum and of the error signal allowed us to estimate the spectral width of stabilised laser radiation to be less than 500 kHz. This radiation is routinely used for cooling atoms on a 10-MHz-wide transition, and the frequency instability for a time interval of 1 s–1 day does not exceed 1 MHz. Hence, in determining the frequency difference for the two transitions, the frequency error for each of them, related to the wavelength metre, is at most 5 MHz. Note that inaccuracy of the absolute value of the transition frequency is 100 MHz.

No frequency shift dependence on the power of 402-nm radiation was observed within the error of 3 MHz.

Due to the Stark effect, the optical lattice can shift positions of the levels |r, 4⟩ and |r, 3⟩; however, one should bear in mind that we deal with two hyperfine components of the same level. The level polarisability that determines the shift value comprises scalar and tensor components, the scalar part being independent of the total atomic moment F. A contribution of the tensor component turns to zero after averaging over all magnetic sublevels. As a result, the polarisabilities of the two studied levels are equal; hence, the frequency shifts are equal at the same intensity of the optical lattice.

For estimating the frequency shift due to the Zeeman effect, the residual magnetic field was found experimentally from the shift of an atomic cloud in MOT under varying gradient of the quadruple field in the trap. The characteristic value of the magnetic field gradient in MOT is 5 Gs cm^{-1}. At a half gradient, the position of the atomic cloud remained constant within the accuracy of 30 μm (the position was determined using the camera), which limits the residual magnetic field to the value of less than 7 mGs. Taking into account g-factors of the levels |c⟩ and |r⟩, such field leads to the frequency difference between outer magnetic sublevels of at most 100 kHz; hence, an estimate of the upper boundary of the frequency error due to the magnetic field yields the value of 0.1 MHz. Below, the values of the error (in MHz) of determining the hyperfine splitting are given for various sources.

Systematic error of the wavelength metre	5
Stark effect (optical lattice)	0
Stark effect (λ = 402 nm)	3
Zeeman effect (residual magnetic field)	0.1
Sum systematic error for each transition	6
Statistical error for the |c, 3⟩ → |r, 4⟩	0.7
Statistical error for the |c, 3⟩ → |r, 3⟩	0.5
Total error	9

Finally we obtain that the hyperfine splitting of the |r⟩ level is 1480(9) MHz, the level with F = 4 being lower in energy than the level with F = 3. The frequency of the |c, 3⟩ → |r, 4⟩ transition is 745061.66(10) GHz.

4. Determining the excitation probability for the clock transition

Figure 4 shows a sequence of pulses for determining the excitation probability of the clock transition. It is assumed that by the time the clock pulse starts, a constant magnetic field is switched on and atoms are optically pumped to the central magnetic sublevel (the procedure is thoroughly described in [16]). The laser used in the present work for probing the clock transition is stabilised to a high-Q resonator using the Pound–Drever–Hall locking technique [21] and has the radiation spectrum width of less than 10 Hz, which is confirmed by the transition line with a width of 10 Hz measured in [10].

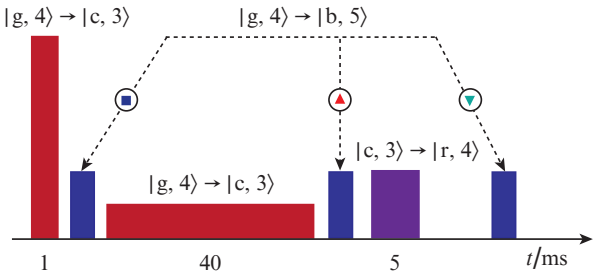

Figure 4. Pulse sequence in the experiment: after a short clock pulse $|g, 4\rangle \rightarrow |c, 3\rangle$, the number n_1 of atoms is detected, which have not been pumped to the central sublevel; then, after a long clock pulse $|g, 4\rangle \rightarrow |c, 3\rangle$, the number n_2 of atoms that have returned to the ground state is measured; finally, by using repumping radiation, the number n_3 of atoms remaining at the upper level of the clock transition is found.

First, a short π-pulse of the clock laser excites nearly all atoms from the central magnetic sublevel. At a duration τ = 1 ms, the transform limited profile width is $\Delta\nu \approx 0.8$ kHz, according to the equation $\Delta\nu\tau \approx 0.8$ for a rectangular pulse. The line width of 1.14 μm laser radiation and the line width of the clock transition are much less than this value. All atoms that remained at the ground level were at a non-zero magnetic sublevel, which is explained by imperfect optical pumping. Due to excitation by a subsequent radiation pulse at 410 nm, these atoms escape from the trap. The camera detects luminescence and the number of atoms n_1 is found which gives an estimate of the optical pumping efficiency ~70%.

Then a long π-pulse of the clock laser follows, which transfers atoms to the ground state. In this experiment, the duration of this pulse was 40 ms, which corresponds to the transform limited line width of approximately 20 Hz. The number of atoms n_2, which have transferred to the ground state is measured in 1 ms after the spectroscopic (long) pulse has passed; in this process, atoms are heated and leave the trap. A delay between the pulses is added to avoid possible overlapping with the clock laser pulse.

Then a radiation pulse of duration 5 ms at a wavelength of 402 nm resonant to the $|c, 3\rangle \rightarrow |r, 4\rangle$ transition is used, which transfers atoms from the upper clock level to the ground state, and then the number of atoms n_3 is finally measured. The pulse duration chosen experimentally is definitely longer than the time needed for the population repumping. Efficiency of the population transfer $k \approx 0.89$ was found experimentally using the fact that the number of atoms in the trap determined as $n_1 + n_2 + n_3/k$ should not depend on the detuning $\Delta\nu$ of the clock radiation frequency from resonance frequency. The excitation probability is found from the last two measurements taking into account the population transfer efficiency

$$p = \frac{n_2}{n_2 + n_3/k}. \qquad (2)$$

Probability p reaches the value of 0.94; however, there is a plateau at a level of 0.35 (Fig. 5). This is related to the fact that during the clock laser radiation pulse of duration 40 ms, some atoms spontaneously decay to the ground state regardless of the pulse presence. This decay occurs regardless of the method of exciting the transition and limits the amplitude of a line profile. Thus, for atom excitation from the ground level with the same experimental parameters the maximal probability p would be 0.6 with a zero-level plateau.

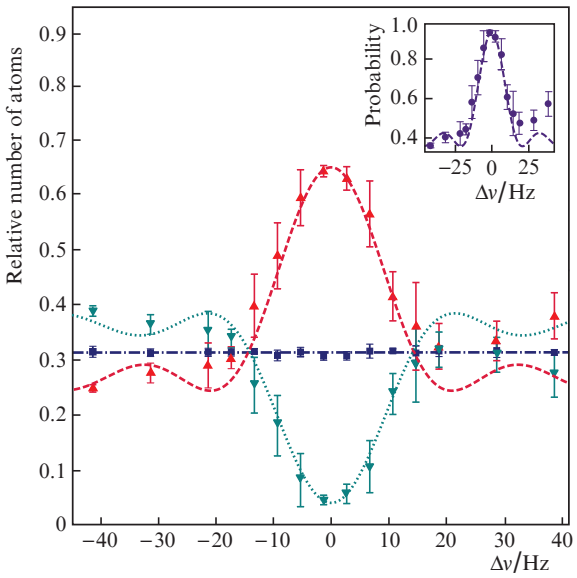

Figure 5. Probability of exciting the clock transition vs. laser radiation frequency detuning from the resonance frequency: relative numbers of atoms n_1, n_2 and n_3 detected as a result of the first (■), second (▲), and third (▼) pulses of illuminating radiation $|g, 4\rangle \rightarrow |b, 5\rangle$, respectively. The inset shows the spectrum of probability p obtained from these numbers by formula (2). Dotted and dashed curves are approximations by the theoretical profile obtained for excitation of the transition by a rectangular pulse.

5. Conclusions

In experiments, the frequency is determined for the transition $|4f^{13}(^2F^o)6s^2;\ J = 5/2,\ F = 3\rangle \rightarrow |4f^{12}(^3F_2)5d_{5/2}6s^2;\ J = 7/2,\ F = 4\rangle\ \nu_{34} = 745061.66(10)$ GHz and the value of hyperfine splitting for the upper level of this transition $\Delta\nu_{hfs}$ = 1480(9) MHz. The transition is used to transfer the population of the upper level of the clock transition to the ground level in a short time not using the clock laser radiation. The method suggested allows one to determine the excitation probability of the clock transition free of fluctuations in the number of atoms in the optical lattice. The profile of excitation probability for a clock transition with a FWHM of 20 Hz is obtained, which demonstrates experimental applications of the method.

Importantly, the radiation shifted in frequency by –653 MHz will help realise the population transfer from the clock sublevel $|4f^{13}(^2F^o)6s^2;\ J = 5/2,\ F = 2\rangle$, which is supposed to be employed for eliminating the quadratic Zeeman effect [10].

Acknowledgements. The work was supported by the Russian Science Foundation (Grant No. 19-72-00174).

References

1. Sanner C., Huntemann N., Lange R., Tamm C., Peik E., Safronova M.S., Porsev S.G. *Nature*, **567**, 204 (2019).

2. Safronova M.S., Porsev S.G., Sanner C., Ye J. *Phys. Rev. Lett*., **20** (17), 173001 (2018).
3. Derevianko A., Pospelov M. *Nature Phys*., **10** (12), 933 (2014).
4. Grotti J., Koller S., Vogt S., Höafner S., Sterr U., Lisdat C., Denker H., Voigt C., Timmen L., Rolland A., et al. *Nature Phys*., **14** (5), 437 (2018).
5. Brewer S.M., Chen J.S., Hankin A.M., Clements E.R., et al. *Phys. Rev. Lett*., **123** (3), 033201 (2019).
6. Bloom B.J., Nicholson T.L., Williams J.R., Campbell S.L., Bishof M., Zhang X., Zhang W., Bromley S.L., Ye J. *Nature*, **506**, 71 (2014).
7. Oelker E., Hutson R.B., Kennedy C.J., Sonderhouse L., Bothwell T., Goban A., Kedar D., Sanner C., Robinson J.M., Marti G.E., Matei D.G. *Nat. Photonics*, **13** (10), 714 (2019).
8. Margolis H.S., Denker H., Voigt C., Timmen L., Grotti J., Koller S., Vogt S., Häfner S., Sterr U., Lisdat C., Rolland A. *Proc. Eur. Conf. on Lasers and Electro-Optics* (Munich, 2019) pp 1–2.
9. Semerikov I.A., Khabarova K.Y., Zalivako I.V., Borisenko A.S., Kolachevsky N.N. *Bull. Lebedev Phys. Inst*., **45** (11), 337 (2018).
10. Golovizin A., Fedorova E., Tregubov D., Sukachev D., Khabarova K., Sorokin V., Kolachevsky N. *Nat. Commun*., **10** (1), 1724 (2019).
11. Beloy K., Hinkley N., Phillips N.B., Sherman J.A., Schioppo M., Lehman J., Feldman A., Hanssen L.M., Oates C.W., Ludlow A.D. *Phys. Rev. Lett*., **113** (26), 260801 (2014).
12. Ushijima I., Takamoto M., Das M., Ohkubo T., Katori H. *Nat. Photonics*, **9** (3), 185 (2015).
13. Ludlow A.D., Boyd M.M., Ye J., Peik E., Schmidt P.O. *Rev. Mod. Phys*., **87** (2), 637 (2015).
14. Kalganova E.S., Golovizin A.A., Shevnin D.O., Tregubov D.O., Khabarova K.Yu., Sorokin V.N., Kolachevsky N.N. *Quantum Electron*., **48** (5), 415 (2018) [*Kvantovaya Elektron*., **48** (5), 415 (2018)].
15. Tregubov D.O., Golovizin A.A., Fedorova E.S., Khabarova K.Yu., Sorokin V.N., Kolachevsky N.N. *Quantum Electron*., **49** (11), 1028 (2019) [*Kvantovaya Elektron*., **49** (11), 1028 (2019)].
16. Fedorova E.S., Tregubov D.O., Golovizin A.A., Vishnyakova G.A., Mishin D.A., Provorchenko D.I., Khabarova K.Yu., Sorokin V.N., Kolachevsky N.N. *Quantum Electron*., **49** (5), 418 (2019) [*Kvantovaya Elektron*., **49** (5), 418 (2019)].
17. Al-Masoudi A., Dörscher S., Häfner S., Sterr U., Lisdat C. *Phys. Rev. A*, **92** (6), 063814 (2015).
18. Hinkley N., Sherman J.A., Phillips N.B., Schioppo M., Lemke N.D., Beloy K., Pizzocaro M., Oates C.W., Ludlow A.D. *Science*, **341** (6151), 1215 (2013).
19. Guena J., Abgrall M., Rovera D., Laurent P., et al. *IEEE Trans. Ultrason. Ferroelec. Freq. Contr*., **59** (3), 391 (2012).
20. Kramida A., Ralchenko Yu., Reader J. NIST ASD Team. NIST Atomic Spectra Database (ver. 5.7.1); https://physics.nist.gov/asd, (2020).
21. Drever R.W., Hall J.L., Kowalski F.V., Hough J., Ford G.M., Munley A.J., Ward H. *Appl. Phys. B*, **31** (2), 97 (1983).